DR-APPENDIX 1. GEOCHRONOLOGY METHODOLOGY

The geochronology methodologies used in this study follow Meffre et al. (2007) for zircon and Berry et al. (2007) for monazite. These analytical techniques are further detailed below.

Zircon geochronology

Dredge samples were crushed in a Cr-steel ring mill and repeatedly sieved to a grain size of >300 μm. Zircons were separated from the heavy mineral separate using warm water, a hand pan and a magnet, mounted in epoxy resin discs and polished so as just to expose the central portions of the grains. Individual zircons were imaged using the cathodoluminescence (CL) technique to reveal detailed internal structure and zonation. These images provided a guide for targeted analyses, so that analyses of 'mixed' growth/recrystallization zones were avoided.

Zircon analyses were performed on a 193 nm New Wave laser coupled to an Agilent 7500 quadrupole ICPMS at the University of Tasmania. Analyses were performed ~2-3 hours after ignition of the LA-ICPMS to enable the machine to stabilise. Four primary standards (Temora) and two secondary standards (91500) were analysed at the beginning of every session and between each 'run' of 12 unknown zircons to correct for mass bias, machine drift and down hole fractionation. Instrument calibrations were checked regularly using Temora (416.8 ± 1.1 Ma; Black et al., 2003) and 91500 (1065 ± 0.4 Ma; Wiedenbeck et al., 1995), which yielded $^{206}Pb/^{238}U$ ages of 415.6 ± 1.4 Ma and 1067.4 ± 6.7 Ma respectively. Zircons were ablated in a He atmosphere in a custom-made chamber using a laser at 5 Hz and a 35 μm diameter beam delivering a density of approximately 3 J/cm^2. Each analysis began with a 30 second blank gas measurement before a further 30 seconds of laser ablation analysis time. Elements measured were ^{96}Zr, ^{146}Nd, ^{178}Hf, ^{202}Hg, ^{204}Pb, ^{206}Pb, ^{207}Pb, ^{208}Pb, ^{232}Th and ^{238}U.

The data reduction method used was based on the method outlined in detail by Black et al. (2004), modified to suite the LA-ICPMS at the University of Tasmania. Average background count rates were subtracted from each isotope and Pb and U isotopic ratios were then calculated for each 0.2 second measurement. Ratios were filtered such that the top and bottom 1% of the data was excluded (to eliminate spikes). Machine drift was calculated via a linear fit to the primary standard data, and checked against the secondary standard. Downhole fractionation and mass bias correction factors were calculated by averaging the drift corrected ratios on each 0.2 second interval of the primary standard measurements (relative to the start of the analysis), calculating a curve fit to the data and normalising to the recommended value for the primary standard. A set of correction factors was generated for each 0.2 second interval and for each isotopic ratio.

Once filtered data was corrected for machine drift, downhole fractionation and mass bias as outlined above, radiometric ages were calculated for each 0.2 second measurement and plotted against the analysis time. An integration interval was then chosen for the most stable part of the analysis in order to exclude contamination from inclusions, and zones of Pb-loss. Due to the low count rates of ^{207}Pb in natural zircon, the instrument bias between ^{207}Pb and ^{206}Pb was determined using analyses on silicate glass standard NIST612 (Baker et al., 2004). The standard errors quoted are based on the standard error of the measurements within the integration intervals and the errors on the measurement of the standards. Element abundances were calculated using the method outlined in Kosler and Sylvester (2003) by assuming stoichiometric Zr as the internal standard element and using the secondary standard to correct for mass bias.

Tera-Wasserburg plots and age calculations were made using Isoplot v.3 (Ludwig, 2003). Uncertainties for individual analyses as quoted in tables and as error bars on zircon plots have been calculated to the one-sigma level. Intercept and weighted mean ages are reported at the 95% confidence level.

Monazite geochronology

Monazite grains in standard thin sections were analysed *in situ* using a Cameca SX100 electron microprobe equipped with five wavelength dispersive spectrometers and operating conditions of 20 kV and 100 nA at the University of Tasmania. The errors quoted are estimated from counting statistics however two additional sources of error need to be considered: (1), Pb background and (2) U background. The Pb background is estimated using a curved background model based on two points measured far away from the Pb peak position. Experiments using pure phases indicate this adds an additional component to the background error of 0.25% of the background counts. In addition, U background is estimated using a constant slope calculation from a measurement on only one side of the peak. This slope is dependent on the mean atomic number of monazite which can vary by up to 2%. Experiments on pure metals indicate that this produces a 1% variation in the slope of the regression. These additional sources of error are included in the calculated standard deviation of Pb and U and these errors have been propagated through the age calculation using the rules for normally distributed errors (Barford, 1985). They do not include any systematic errors associated with calibration, or the errors in the decay constants. Instrument calibrations were checked regularly using standard monazite grains including RGL4B (1566 ± 3 Ma; Rubatto et al., 2001) and 94–222 (467 ± 8 Ma; Hand et al., 1999) and yielded ages of 1576 ± 11 Ma and 473 ± 6 Ma respectively. Several internal standards were also used. Based on these results a best estimate of the systematic error is +0.7 ± 0.7 %, that is the ages reported in this manuscript are probably high by an amount in the range 0 to 7 Myr and must be considered when these ages are compared against ages from other laboratories and using other techniques.

In addition to U, Pb and Th we analysed Si, Al, K, Fe, Ca, Sr, Y, La, Ce, Pr, Nd, Sm, Eu, Gd, Dy, Yb, Er, P, S and As. The Si, Al and K contents was used to identify contaminated analyses. The assessment of K content for each analysis is critical, since the U analysis is very sensitive to interference from K. All analyses used for age calculations were screened closely based on stoichiometric, oxide totals and contaminating elements to remove inferior results. Weighted mean ages were calculated using Isoplot v.3 (Ludwig, 2003). Uncertainties for individual analyses are one-sigma. Weighted mean ages are reported at the 95% confidence level.

REFERENCES

Baker, J., Peate, D., Waight, T., and Meyzen, C., 2004, Pb isotopic analysis of standards and samples using a Pb-207-Pb-204 double spike and thallium to correct for mass bias with a double-focusing MC-ICP-MS: Chemical Geology, v. 211, p. 275-303.

Barford, N.C., 1985, Experimental measurements: precision, error, and truth: Chichester, Wiley, 159 p.

Berry, R.F., Chmielowski, R.M., Steele, D.A., and Meffre, S., 2007, Chemical U-Th-Pb monazite dating of the Cambrian Tyennan Orogeny, Tasmania: Australian Journal of Earth Sciences, v. 54, p. 757 - 771.

Black, L.P., Kamo, S.L., Allen, C.M., Aleinikoff, J.N., Davis, D.W., Korsch, R.J., and Foudoulis, C., 2003, TEMORA 1: a new zircon standard for Phanerozoic U-Pb geochronology: Chemical Geology, v. 200, p. 155–170.

Black, L.P., Kamo, S.L., Allen, C.M., Davis, D.W., Aleinikoff, J.N., Valley, J.W., Mundil, R., Campbell, I.H., Korsch, R.J., Williams, I.S., and Foudoulis, C., 2004, Improved 206Pb-206/U-218 microprobe geochronology by the monitoring of a trace-element-related matrix effect; SHRIMP, ID-TIMS, ELA-ICP-MS and oxygen isotope documentation for a series of zircon standards: Chemical Geology, v. 205, p. 115-140.

Hand, M., Mawby, J., Kinny, P., and Foden, J., 1999, U-Pb ages from the Harts Range, central Australia: evidence for early Ordovician extension and constraints on Carboniferous metamorphism: Journal of the Geological Society, v. 156, p. 715–730.

Kosler, J., and Sylvester, P.J., 2003, Present trends and the future of zircon in geochronology: Laser ablation ICPMS, Zircon, Volume 53: Reviews in Mineralogy & Geochemistry, p. 243-275.

Ludwig, K.R., 2003, Isoplot 3.00: A Geochronological Toolkit for Microsoft Excel, Berkeley Geochronological Centre Special Publication no. 4.

Meffre, S., Scott, R.J., Glen, R.A., and Squire, R.J., 2007, Re-evaluation of contact relationships between Ordovician volcanic belts and the quartz-rich turbidites of the Lachlan Orogen: Australian Journal of Earth Sciences, v. 54, p. 363 - 383.

Rubatto, D., Williams, I.S., and Buick, I.S., 2001, Zircon and monazite response to prograde metamorphism in the Reynolds Range, central Australia: Contributions to Mineralogy and Petrology, v. 140, p. 458–468.

Wiedenbeck, M., Alle, P., Corfu, F., Griffin, W.L., Meier, M., Oberli, F., Vonquadt, A., Roddick, J.C., and Speigel, W., 1995, 3 Natural Zircon Standards for U-Th-Pb, Lu-Hf, Trace-Element and REE Analyses: Geostandards Newsletter, v. 19, p. 1–23.

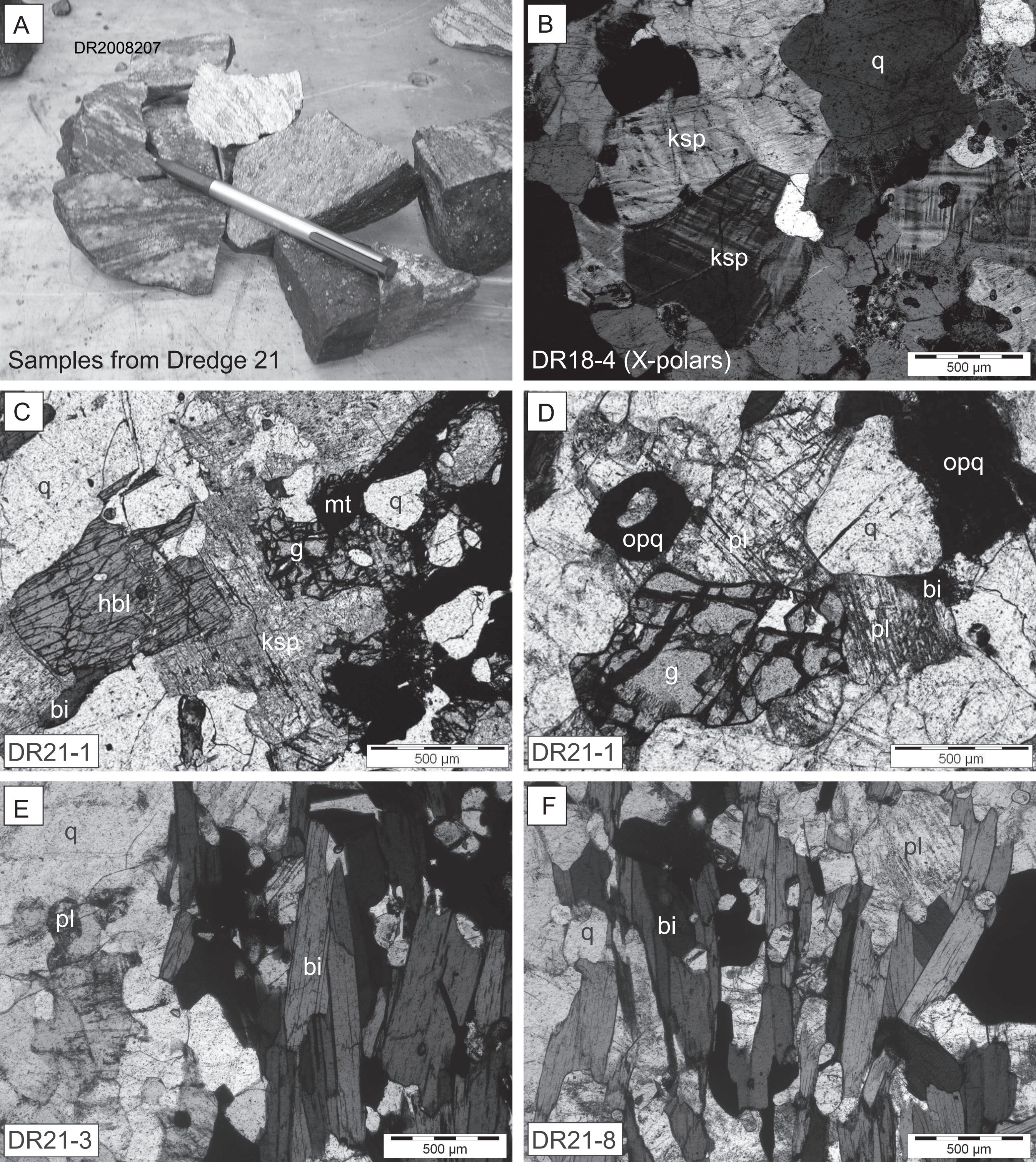

Data Repository Figure 1.

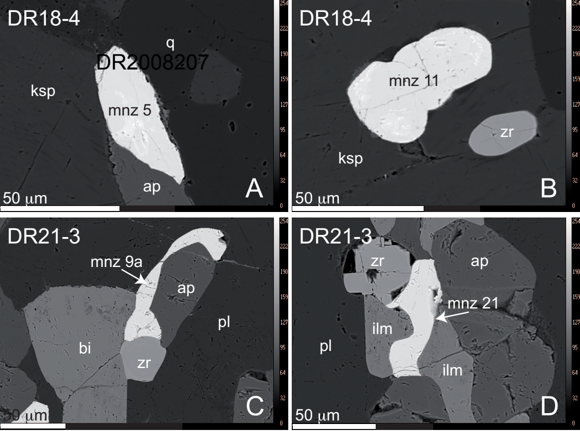

Data Repository Figure 2.

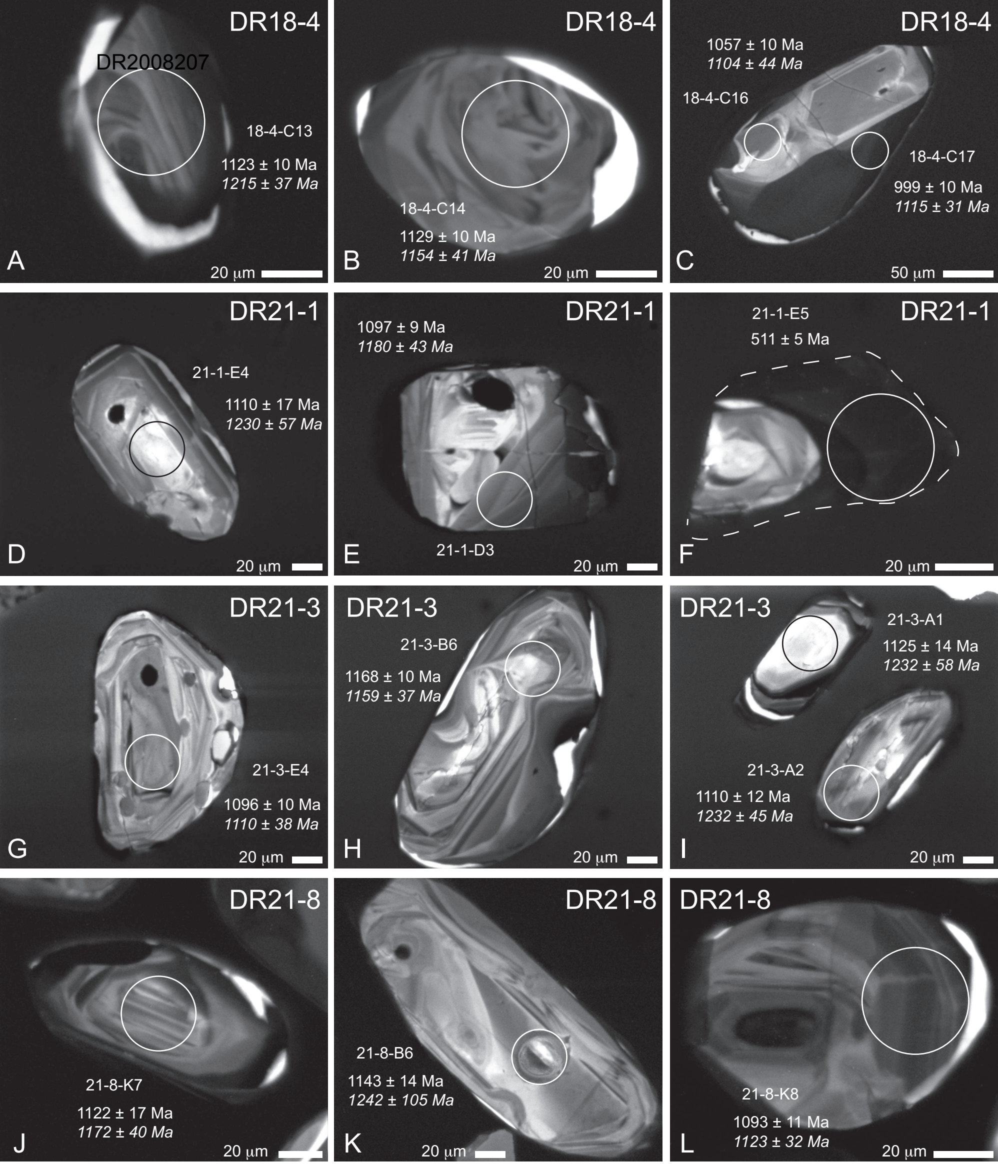

Data Repository Figure 3.

DATA REPOSITORY CAPTIONS

DR-Fig. 1. (a) Photograph of representative gneissic fragments from dredge 21 from the Naturaliste Plateau. Photomicrographs of mineral assemblages from (b) microcline-phyric coarse granite sample DR18-4, (c)-(d) gneissic quartz diorite sample DR21-1, (e) felsic orthogneiss sample DR21-3 and (f) felsic orthogneiss sample DR21-8. Mineral abbreviations: bi; biotite, g; garnet, hbl; hornblende, ksp; K-feldspar, mt; magnetite, opq; opaque mineral (ilmenite or magnetite), pl; plagioclase, q; quartz.

DR-Fig. 2. Backscattered electron (BSE) images of monazites from (a)-(b) sample DR18-4 and (c)-(d) sample DR21-3. Additional mineral abbreviations: ap; apatite, ilm; ilmenite, mnz; monazite, zrc; zircon.

DR-Fig. 3. Representative cathodoluminescence (CL) images of zircons from (a)-(c) sample DR18-4, (d)-(f) sample DR21-1, (g)-(i) sample DR21-3 and (j)-(k) sample DR21-8. $^{206}Pb/^{238}U$ ages are shown in italics. Ages are quoted with one-sigma errors. Analysis spots are shown to scale.

TABLE 1. COMPILATION OF U-PB ZIRCON DATA FROM EAST GONDWANA (WESTERN AUSTRALIA AND EAST ANTARCTICA) FOR FIG. 1

Age* (Ma)	+/- ☐	Tech.§	Sample no.	Rock type	Region#	Orogen**	Event/age interpretation	Reference
514	7	S	31	foliated granite	SPB	PBDG	emplacement	Carson et al. 1996
516	7	S	261	foliated granite	SPB	PBDG	emplacement	Carson et al. 1996
535	13	S	88/105	foliated garnet leucogneiss	SPB	PBDG	emplacement	Fitzsimons et al. 1997
536	35	S	88/122	foliated leucogneiss	SPB	PBDG	emplacement	Fitzsimons et al. 1997
540	19	S	SP12	granitic orthogneiss	RG	PBDG	metamorphism	Kinny et al. 1993
489	6	S	TI13	granitic orthogneiss	RG	PBDG	metamorphism	Kinny et al. 1993
498	28	S	TI14	paragneiss	RG	PBDG	metamorphism	Kinny et al. 1993
504	14	S	TI14	paragneiss	RG	PBDG	metamorphism	Kinny et al. 1993
1027	27	S	F104	granite gneiss	RG	PBDG	crystallization	Kinny et al. 1993
1057	22	S	FI02	leucosome	RG	PBDG	migmatization	Kinny et al. 1993
998	18	S	FI05	garnet leucogneiss	RG	PBDG	emplacement	Kinny et al. 1993
548	26	S	FI06	aplitic leucogneiss	RG	PBDG	metamorphism	Kinny et al. 1993
500	12	S	FI03	pegmatite	RG	PBDG	crystallization	Kinny et al. 1993
511	10	S	RI43	diorite	RG	PBDG	metamorphism	Kinny et al. 1993
512	12	S	RI15	grt-qtz rock	RG	PBDG	metamorphism	Kinny et al. 1993
528	12	S	SH45	tonalitic orthogneiss	RG	PBDG	metamorphism	Kinny et al. 1993
513	2	S	86286024	syenite	DG	PBDG	emplacement	Black et al. 1992a
567	49	S	86285893	tonalitic orthogneiss	DG	PBDG	metamorphism	Black et al. 1992a
922	32	S	ZR1-1	felsic orthogneiss	GM	PBDG	emplacement	Liu et al. 2007
914	17	S	MP1-7	felsic orthogneiss	GM	PBDG	emplacement	Liu et al. 2007
536	8	S	MP1-7	felsic orthogneiss	GM	PBDG	metamorphism	Liu et al. 2007
910	14	S	HM1-5	felsic orthogneiss	GM	PBDG	emplacement	Liu et al. 2007
907	21	S	ZR1-2	mafic granulite	GM	PBDG	emplacement	Liu et al. 2007
545	9	S	ZR1-2	mafic granulite	GM	PBDG	metamorphism	Liu et al. 2007
549	8	S	MP2-4	mafic granulite	GM	PBDG	metamorphism	Liu et al. 2007
548	9	S	MN1-1	mafic granulite	GM	PBDG	metamorphism	Liu et al. 2007
475	29	S	BP2-3	paragneiss	GM	PBDG	metamorphism	Liu et al. 2007
1174	26	S	72-7	orthogneiss	McK	PBDG	emplacement	Liu et al. 2007b
529	11	S	72-7	orthogneiss	McK	PBDG	metamorphism	Liu et al. 2007b
1137	46	S	72-1	mafic granulite	McK	PBDG	emplacement	Liu et al. 2007b
1019	33	S	80-1	garnet-bearing mafic granulite	McK	PBDG	emplacement	Liu et al. 2007b
533	9	S	80-1	garnet-bearing mafic granulite	McK	PBDG	metamorphism	Liu et al. 2007b
533	10	S	71-1	paragneiss	McK	PBDG	metamorphism	Liu et al. 2007b
537	7	C	W203	felsic granulite	LC	PO	emplacement	Wilde and Murphy 1990
564	4	C	W203	felsic granulite	LC	PO	emplacement	Wilde and Murphy 1990

TABLE 1. *CONTINUED*

Age* (Ma)	+/- □	Tech.§	Sample no.	Rock type	Region#	Orogen**	Event/age interpretation	Reference
549	15	C	W203	felsic granulite	LC	PO	emplacement	Wilde and Murphy 1990
779	23	S	112134	granitic gneiss	LC	PO	crystallization	Nelson 1996
605	36	S	112134	granitic gneiss	LC	PO	remelting/metamorphism	Nelson 1996
688	7	S	112132	granitic gneiss	LC	PO	crystallization	Nelson 1996
681	10	S	112131	granitic augen gneiss	LC	PO	crystallization	Nelson 1996
702	7	S	112144	granitic augen gneiss	LC	PO	crystallization	Nelson 1996
625	14	S	112144	granitic augen gneiss	LC	PO	metamorphism	Nelson 1996
540	6	S	112143	granite	LC	PO	crystallization	Nelson 1996
524	12	S	112140	granite dyke	LC	PO	crystallization	Nelson 1996
1091	8	S	112135	monzogranitic augen gneiss	LC	PO	crystallization	Nelson 1999
1016	10	S	112135	monzogranitic augen gneiss	LC	PO	lead loss	Nelson 1999
1091	17	S	121136	monzogranitic augen gneiss	LC	PO	crystallization	Nelson 1999
1005	46	S	121136	monzogranitic augen gneiss	LC	PO	lead loss	Nelson 1999
535	9	S	112145	aegirine-augite syenite gneiss	LC	PO	crystallization	Nelson 1999
746	15	S	SL05	granite gneiss	LC	PO	crystallization	Collins 2003
522	5	S	SL01	granodiorite gneiss	LC	PO	metamorphism	Collins 2003
730	11	S	169002	bi-hbl-cpx-mt syenogranite gneiss	LC	PO	crystallization	Nelson 2002
542	28	S	169002	bi-hbl-cpx-mt syenogranite gneiss	LC	PO	metamorphism	Nelson 2002
515	19	S	169001	bi-hbl-cpx syenogranite gneiss	LC	PO	metamorphism	Nelson 2002
1079	3	C	W405	mafic granulite	NC	PO	metamorphism	Bruguier et al. 1999
1059	32	S	W404	psammitic paragneiss	NC	PO	metamorphism	Bruguier et al. 1999
1068	13	S	W412	porphyritic granite	NC	PO	crystallization	Bruguier et al. 1999
989	2	C	W411	pegmatite	NC	PO	crystallization	Bruguier et al. 1999
1521	29	S	86285628	granodioritic orthogneiss	BH	WO	emplacement	Sheraton et al. 1992
1190	15	S	86285628	granodioritic orthogneiss	BH	WO	metamorphism	Sheraton et al. 1992
1171	3	S	86285962	quartz monzo gabbro	BH	WO	crystallization	Sheraton et al. 1992
1170	4	S	86286245	quartz monzo gabbro	BH	WO	crystallization	Sheraton et al. 1992
1151	4	S	86285815	quartz monzodiorite	BH	WO	crystallization	Sheraton et al. 1992
1275	21	C	786-T38	grt-opx paragneiss	WI	WO	metamorphism	Oliver et al. 1983
1340	50	S	See note	Not known	WI	WO	metamorphism	Post et al. 1997
1180	50	S	See note	Not known	WI	WO	metamorphism	Post et al. 1997
1170	50	S	See note	granite	WI	WO	crystallization	Post et al. 1997
1160	50	S	See note	charnockite	WI	WO	crystallization	Post et al. 1997
1135	50	S	See note	aplite	WI	WO	crystallization	Post et al. 1997
1174	12	C	W139	adamellite	AF	AFO	emplacement	Pidgeon 1990

TABLE 1. *CONTINUED*

Age* (Ma)	+/- ☐	Tech.§	Sample no.	Rock type	Region#	Orogen**	Event/age interpretation	Reference
1177	4	C	W140	adamellite	AF	AFO	emplacement	Pidgeon 1990
1289	10	C	W141	enderbite gneiss	AF	AFO	emplacement	Pidgeon 1990
1196	8	S	AFP1	opx-hbl-pl pegmatite	AF	AFO	crystallization	Black et al. 1992b
1189	9	S	MF2	granite	AF	AFO	crystallization	Black et al. 1992b
1182	12	S	AFP8	aplite dyke	AF	AFO	crystallization	Black et al. 1992b
1184	11	S	AFP9	granitic augen gneiss	AF	AFO	crystallization	Black et al. 1992b
1180	6	S	AFP2	pegmatite in felsic orthogneiss	AF	AFO	crystallization	Black et al. 1992b
1299	14	S	83690	biotite granodiorite gneiss	AF	AFO	crystallization	Nelson et al. 1995
1187	12	S	83649	granite pegmatite	AF	AFO	crystallization	Nelson et al. 1995
1283	13	S	83700A	hbl-bi granite gneiss	AF	AFO	crystallization	Nelson et al. 1995
1299	18	S	83697	biotite monzogranite augen gneis	AF	AFO	crystallization	Nelson et al. 1995
1288	12	S	83659	leucogranite gneiss	AF	AFO	crystallization	Nelson et al. 1995
1138	38	S	83657A	biotite monzogranite	AF	AFO	crystallization	Nelson et al. 1995
1330	14	S	83662	bi-hbl monzogranite gneiss	AF	AFO	crystallization	Nelson et al. 1995
1314	21	S	83663	biotite granodiorite gneiss	AF	AFO	crystallization	Nelson et al. 1995
1301	6	S	MM-1	charnockite	AF	AFO	crystallization	Clark et al. 1999
1293	9	S	FR-1	orthopyroxene granite	AF	AFO	crystallization	Clark et al. 1999
1288	12	S	GH-1	aplite dyke	AF	AFO	crystallization	Clark et al. 1999
1313	16	S	95091214	aplite dyke	AF	AFO	crystallization	Clark et al. 2000
1313	16	S	9509243	aplite dyke	AF	AFO	crystallization	Clark et al. 2000
1214	8	S	9611201	leucosome	AF	AFO	crystallization	Clark et al. 2000
1182	13	S	9611201	leucosome	AF	AFO	deformation/fluid flow	Clark et al. 2000
1226	36	S	DR21-8	felsic orthogneiss	NP	NP	emplacement	this study
1198	44	S	DR18-4	granite gneiss	NP	NP	emplacement	this study
1185	32	S	DR21-3	felsic orthogneiss	NP	NP	emplacement	this study
1178	40	S	DR21-1	felsic orthogneiss	NP	NP	emplacement	this study

Note: No errors or sample numbers are reported by Post et al. (1997), so an error of 50 Myr has been assigned.
*ages >1600 Ma, <450 Ma and ages of detrital grains or xenocrysts are excluded.
☐ages with errors (at 95% confidence) of greater than 50 Myr are excluded.
§technique: C = conventional U-Pb analysis by zircon dissolution; S = U-Pb ion probe analysis (SHRIMP or LA-ICPMS)
#regions: AF = Albany Fraser; BH = Bunger Hills; DG = Denman Glacier; GM = Grove Mountains; LC = Leeuwin Complex; McK = McKaskle Hills; NC = Northampton Complex; NP = Naturaliste Plateau; RG = Rauer Group; SPB = Southern Prydz Bay; WI = Windmill Islands.
**orogen/province (corresponding to Fig. 1): AFO, Albany-Fraser Orogen; NP, Naturaliste Plateau; PO, Pinjarra Orogen; PBDG, Prydz Bay-Denman Glacier; WO, Wilkes Orogen.

REFERENCES CITED IN DATA REPOSITORY TABLE 1

Black, L.P., Harris, L.B., and Delor, C.P., 1992a, Reworking of Archaean and Early Proterozoic components during a progressive, Middle Proterozoic tectonothermal event in the Albany Mobile Belt, Western Australia: Precambrian Research, v. 59, p. 95-123.

Black, L.P., Sheraton, J.W., Tingey, R.J., and McCulloch, M.T., 1992b, New U-Pb zircon ages from the Denman Glacier area, East Antarctica, and their significance for Gondwana reconstruction: Antarctic Science, v. 4, p. 447-460.

Bruguier, O., Bosch, D., Pidgeon, R.T., Byrne, D.I., and Harris, L.B., 1999, U-Pb chronology of the Northampton Complex, Western Australia - evidence for Grenvillian sedimentation, metamorphism and deformation and geodynamic implications: Contributions to Mineralogy and Petrology, v. 136, p. 258-272.

Carson, C.J., Fanning, C.M., and Wilson, C.J.L., 1996, Timing of the Progress Granite, Larsemann Hills: additional evidence for Early Palaeozoic orogenesis within the East Antarctic Shield and implications for Gondwana assembly: Australian Journal of Earth Sciences, v. 43, p. 539-553.

Clark, D.J., Hensen, B.J., and Kinny, P.D., 2000, Geochronological constraints for a two-stage history of the Albany-Fraser Orogen, Western Australia: Precambrian Research, v. 102, p. 155-183.

Clark, D.J., Kinny, P.D., Post, N.J., and Hensen, B.J., 1999, Relationships between magmatism, metamorphism and deformation in the Fraser Complex, Western Australia: constraints from new SHRIMP U-Pb zircon geochronology: Australian Journal of Earth Sciences, v. 46, p. 923-932.

Collins, A.S., 2003, Structure and age of the northern Leeuwin Complex, Western Australia: constraints from field mapping and U-Pb isotopic analysis: Australian Journal of Earth Sciences, v. 50, p. 585-599.

Fitzsimons, I.C.W., Kinny, P.D., and Harley, S.L., 1997, Two stages of zircon and monazite growth in anatectic leucogneiss: SHRIMP constraints on the duration and intensity of Pan-African metamorphism in Prydz Bay, East Antarctica: Terra Nova, v. 9, p. 47-51.

Kinny, P.D., Black, L.P., and Sheraton, J.W., 1993, Zircon Ages and the Distribution of Archean and Proterozoic Rocks in the Rauer Islands: Antarctic Science, v. 5, p. 193-206.

Liu, X., Jahn, B.-M., Zhao, Y., Zhao, G., and Liu, X., 2007a, Geochemistry and geochronology of high-grade rocks from the Grove Mountains, East Antarctica: Evidence for an Early Neoproterozoic basement metamorphosed during a single Late Neoproterozoic/Cambrian tectonic cycle: Precambrian Research, v. 158, p. 93-118.

Liu, X., Zhao, Y., Zhao, G., Jian, P., and Xu, G., 2007b, Petrology and Geochronology of Granulites from the McKaskle Hills, Eastern Amery Ice Shelf, Antarctica, and Implications for the Evolution of the Prydz Belt: Journal of Petrology, v. 48, p. 1443-1470.

Nelson, D.R., 1996, Compilation of SHRIMP U-Pb zircon geochronological data, 1995, Geological Survey of Western Australia, Record 1996/5, p. 168.

—, 1999, Compilation of geochronological data, 1998, Geological Survey of Western Australia, Record 1999/2, p. 222.

—, 2002, Compilation of geochronological data, 2001, Geological Survey of Western Australia, Record 2002/2, p. 282.

Nelson, D.R., Myers, J.S., and Nutman, A.P., 1995, Chronology and evolution of the Middle Proterozoic Albany-Fraser Orogen, Western Australia: Australian Journal of Earth Sciences, v. 42, p. 481 - 495.

Oliver, R.L., Cooper, A.F., and Truelove, A.J., 1983, Petrology and zircon geochronology of Herring island and Commonwealth bay and evidence for Gondwana reconstruction, *in* Oliver, R.L., et al., eds., Antarctic Earth Science: Canberra, Australian Academy of Science, p. 64-68.

Pidgeon, R.T., 1990, Timing of plutonism in the Proterozoic Albany Mobile Belt, southwestern Australia: Precambrian Research, v. 47, p. 157-167.

Post, N.J., Hensen, B.J., and Kinny, P.D., 1997, Two metamorphic episodes during a 1340 - 1180 Ma convergent tectonic event in the Windmill Islands, east Antarctica, *in* Ricci, C.A., ed., The Antarctic Region: Geological Evolution and Processes: Siena, Terra Antarctica, p. 157-161.

Sheraton, J.W., Black, L.P., and Tindle, A.G., 1992, Petrogenesis of plutonic rocks in a Proterozoic granulite-facies terrane - the Bunger Hills, East Antarctica: Chemical Geology, v. 97, p. 163-198.

Wilde, S.A., and Murphy, D.M.K., 1990, The nature and origin of Late Proterozoic high-grade gneisses of the Leeuwin Block, Western Australia: Precambrian Research, v. 47, p. 251-270.

TABLE 2. EMP MONAZITE U-TH-PB CHEMICAL DATA

Sample	No	Pb (ppm)	1s	Th (ppm)	1s	U (ppm)	1s	Age (Ma)	1s
DR18-4	1	1894	48	72506	438	2882	108	514	13
DR18-4	2	2453	50	98693	505	1391	76	529	11
DR18-4	3	2403	49	94548	494	2770	101	516	11
DR18-4	4	2462	49	93099	489	3115	101	530	11
DR18-4	5	2453	50	95296	498	2279	95	531	11
DR18-4	6	2005	49	75508	448	3073	109	522	13
DR18-4	7	2784	50	105100	519	3889	110	526	10
DR18-4	8	1857	49	74755	442	2438	103	500	13
DR18-4	9	2164	49	85466	471	2787	104	509	12
DR18-4	10	2240	49	86805	475	3027	107	515	12
DR18-4	11	1773	48	68318	427	2511	107	516	14
DR18-4	12	2037	49	78481	454	2785	106	518	13
DR18-4	13	1448	48	55708	390	2592	111	502	17
DR18-4	14	2567	50	97605	501	3829	111	519	10
DR18-4	15	1826	48	66902	422	2622	107	538	14
DR18-4	16	1908	48	76851	449	1801	93	513	13
DR18-4	17	2336	49	91440	487	1921	90	532	11
DR18-4	18	1508	46	82237	461	2433	96	374	11
DR18-4	19	2360	49	92033	488	2940	104	517	11
DR18-4	20	2432	50	95335	494	3303	108	510	11
DR18-4	21	2228	49	87306	475	3232	108	507	11
DR18-4	22	1138	47	52826	380	1969	105	429	18
DR18-4	23	1848	48	69609	431	2927	112	519	14
DR18-4	24	2194	49	84545	469	2800	106	521	12
DR18-4	25	2797	50	103982	516	3744	109	535	10
DR21-3	1	1987	49	76191	449	2912	110	516	13
DR21-3	2	804	46	33067	313	868	94	498	29
DR21-3	3	841	46	33078	314	1292	105	502	28
DR21-3	4	909	46	35757	324	1220	101	509	26
DR21-3	5	971	46	37651	330	1191	99	520	25
DR21-3	6	1009	46	40037	339	1153	97	513	24
DR21-3	7	858	46	31251	307	1079	101	549	30
DR21-3	8	1054	46	37834	332	1368	103	554	25
DR21-3	9	984	46	36261	324	1416	105	535	25
DR21-3	10	847	46	32711	311	1559	109	499	27
DR21-3	11	972	46	38721	335	1361	102	501	24
DR21-3	12	1015	47	38504	334	1261	100	530	25
DR21-3	13	853	46	32578	311	1104	100	525	29
DR21-3	14	900	46	34313	319	1213	101	523	27
DR21-3	15	740	46	27653	292	823	96	542	34
DR21-3	16	792	46	31449	307	998	98	508	30
DR21-3	17	832	46	31939	310	1013	99	525	29

TABLE 2. *CONTINUED*

Sample	No	Pb (ppm)	1s	Th (ppm)	1s	U (ppm)	1s	Age (Ma)	1s
DR21-3	18	1012	47	38083	333	1296	101	532	25
DR21-3	19	899	46	35425	321	1581	109	493	26
DR21-3	20	965	46	35491	323	1580	107	528	26
DR21-3	21	900	46	32999	312	963	97	553	29
DR21-3	22	850	46	33144	314	1023	97	518	28
DR21-3	23	1050	47	40042	339	1194	96	531	24
DR21-3	24	989	47	37142	329	1437	103	526	25
DR21-3	25	964	46	34323	319	1773	110	535	26
DR21-3	26	942	46	35845	325	1715	109	506	25
DR21-3	27	1042	46	38468	332	2086	112	512	23
DR21-3	28	928	47	38764	334	1100	96	488	25
DR21-3	29	777	46	31515	306	942	96	500	30
DR21-3	30	776	46	29834	300	1086	101	518	31
DR21-3	31	880	46	36688	326	749	85	501	26
DR21-3	32	987	46	37390	329	871	89	545	26
DR21-3	33	788	46	28015	293	1429	109	536	31
DR21-3	34	929	46	36793	329	1203	99	508	26
DR21-3	35	879	46	33352	313	1365	105	517	27
DR21-3	36	844	46	31235	306	1113	101	538	30
DR21-3	37	818	46	32680	311	1095	100	502	29
DR21-3	38	753	46	27071	289	1097	103	546	33
DR21-3	39	714	46	28747	296	1238	105	485	31
DR21-3	40	827	46	34743	320	1304	102	473	27
DR21-3	41	981	46	36342	327	1160	99	544	26
DR21-3	42	1070	47	45019	355	1142	93	489	22
DR21-3	43	897	46	33679	317	911	94	544	28
DR21-3	44	839	46	32448	312	937	96	525	29
DR21-3	45	828	46	31737	308	1026	98	525	29
DR21-3	46	956	47	36493	326	1481	105	515	25
DR21-3	47	1033	46	37909	332	1396	103	541	25
DR21-3	48	899	46	34511	318	1258	102	518	27
DR21-3	49	903	46	33973	317	967	95	541	28

TABLE 3. LA-ICPMS U-PB ZIRCON ISOTOPIC DATA

						Radiogenic Ratios						Age Estimates (Ma)						
Sample	Analysis	U (ppm)	Th (ppm)	$^{232}Th/^{238}U$	comm. Pb^{206} (%)	$^{206}Pb/^{238}U$	1s	$^{207}Pb/^{235}U$	1s	$^{207}Pb/^{206}Pb$	1s	$^{206}Pb/^{238}U$	1s	$^{207}Pb/^{235}U$	1s	$^{207}Pb/^{206}Pb$	1s	conc. (%)
DR18-4	jl04c1	81	169	2.09	-0.06	0.1702	0.0017	1.8654	0.0428	0.0794	0.0019	1013	9	1069	15	1182	48	86
DR18-4	jl04c2	166	187	1.13	0.07	0.1945	0.0016	2.1399	0.0332	0.0797	0.0013	1146	8	1162	11	1190	31	96
DR18-4	jl04c3	179	120	0.67	-0.02	0.1908	0.0021	2.1979	0.0459	0.0835	0.0017	1126	11	1180	15	1281	39	88
DR18-4	jl04c4	120	150	1.26	0.11	0.1937	0.0018	2.1214	0.0396	0.0791	0.0015	1141	10	1156	13	1175	39	97
DR18-4	jl04c5	277	142	0.52	0.00	0.2020	0.0021	2.1925	0.0394	0.0786	0.0015	1186	11	1179	13	1162	38	102
DR18-4	jl04c6	189	197	1.05	-0.01	0.1897	0.0016	2.0652	0.0328	0.0789	0.0013	1120	9	1137	11	1169	33	96
DR18-4	jl04c7	184	325	1.77	0.13	0.1859	0.0017	2.0804	0.0343	0.0804	0.0013	1099	9	1142	11	1207	33	91
DR18-4	jl04c8	108	108	1.00	-0.23	0.1901	0.0023	1.9897	0.0504	0.0767	0.0019	1122	13	1112	17	1113	50	101
DR18-4	jl04c9	44	72	1.62	0.50	0.1910	0.0024	2.1893	0.0611	0.0828	0.0023	1127	13	1178	20	1264	55	89
DR18-4	jl04c10	79	150	1.92	0.40	0.1511	0.0020	1.5216	0.0474	0.0732	0.0026	907	11	939	19	1020	71	89
DR18-4	jl04c11	97	134	1.39	0.07	0.1957	0.0020	2.1618	0.0403	0.0807	0.0015	1152	11	1169	13	1214	37	95
DR18-4	jl04c12	79	123	1.55	-0.20	0.1611	0.0017	1.6854	0.0410	0.0748	0.0019	963	9	1003	16	1063	51	91
DR18-4	jl04c13	143	168	1.19	0.06	0.1902	0.0018	2.1015	0.0378	0.0807	0.0015	1123	10	1149	12	1215	37	92
DR18-4	jl04c14	104	161	1.56	-0.07	0.1915	0.0019	2.0512	0.0394	0.0783	0.0016	1129	10	1133	13	1154	41	98
DR18-4	jl04c15	101	121	1.21	-0.18	0.1854	0.0016	2.0119	0.0371	0.0789	0.0015	1097	9	1120	13	1170	38	94
DR18-4	jl04c16	90	194	2.16	0.40	0.1782	0.0019	1.8647	0.0393	0.0763	0.0017	1057	10	1069	14	1104	44	96
DR18-4	jl04c17	614	155	0.25	-0.03	0.1677	0.0019	1.7810	0.0273	0.0768	0.0012	999	10	1039	10	1115	31	90
DR18-4	jl04c18	81	110	1.36	-0.09	0.1899	0.0028	2.1922	0.0548	0.0836	0.0021	1121	15	1179	18	1283	50	87
DR18-4	JN30A4	122	135	1.05	0.12	0.1986	0.0028	2.0354	0.1042	0.0853	0.0042	1168	15	1127	35	1323	95	88
DR18-4	JN30A5	62	101	1.54	0.02	0.1955	0.0032	1.8824	0.1186	0.0801	0.0049	1151	17	1075	43	1200	121	96
DR18-4	JN30A6	88	106	1.14	-1.98	0.1864	0.0060	1.7073	0.1838	0.0786	0.0080	1102	33	1011	71	1162	203	95
DR18-4	JN30A9	171	260	1.44	0.01	0.2005	0.0026	1.9679	0.0876	0.0808	0.0035	1178	14	1105	30	1217	86	97
DR21-1	JN20d1	27	65	2.22	-0.64	0.1842	0.0026	1.9828	0.0637	0.0788	0.0026	1090	14	1110	22	1167	65	93
DR21-1	JN20d2	61	123	1.90	0.29	0.1819	0.0029	2.0733	0.0773	0.0841	0.0029	1078	16	1140	26	1294	68	83
DR21-1	JN20d3	89	165	1.73	0.06	0.1856	0.0017	2.0477	0.0436	0.0793	0.0017	1097	9	1132	15	1180	43	93
DR21-1	JN20d4	398	642	1.51	-0.01	0.1917	0.0018	2.0608	0.0257	0.0770	0.0010	1131	10	1136	9	1121	25	101
DR21-1	JN20d5	36	76	2.01	0.40	0.1872	0.0025	2.1036	0.0597	0.0807	0.0022	1106	13	1150	20	1214	54	91
DR21-1	JN20d6	107	220	1.92	-0.08	0.1819	0.0018	1.9283	0.0387	0.0763	0.0015	1077	10	1091	14	1103	39	98
DR21-1	JN20d7	34	71	1.99	0.34	0.1879	0.0026	2.0554	0.0645	0.0794	0.0025	1110	14	1134	22	1183	63	94
DR21-1	JN20d8	38	86	2.15	0.13	0.1877	0.0037	1.9951	0.0930	0.0790	0.0041	1109	20	1114	32	1172	103	95
DR21-1	JN20d9	75	157	1.96	0.00	0.1780	0.0048	1.9263	0.0698	0.0796	0.0035	1056	26	1090	25	1188	86	89
DR21-1	JN20d10	60	149	2.30	-0.17	0.1754	0.0026	1.8914	0.0410	0.0775	0.0016	1042	14	1078	15	1134	40	92
DR21-1	JN20d11	90	128	1.34	0.03	0.1911	0.0031	2.4052	0.0511	0.0914	0.0019	1127	17	1244	15	1456	39	77

TABLE 3. *CONTINUED*

						Radiogenic Ratios						Age Estimates (Ma)						
Sample	Analysis	U (ppm)	Th (ppm)	$^{232}Th/^{238}U$	comm. Pb^{206} (%)	$^{206}Pb/^{238}U$	1s	$^{207}Pb/^{235}U$	1s	$^{207}Pb/^{206}Pb$	1s	$^{206}Pb/^{238}U$	1s	$^{207}Pb/^{235}U$	1s	$^{207}Pb/^{206}Pb$	1s	conc. (%)
DR21-1	JN20d12	97	260	2.50	-0.01	0.1963	0.0035	2.0654	0.0646	0.0770	0.0022	1155	19	1137	22	1122	58	103
DR21-1	JN20e1	46	77	1.54	0.08	0.1841	0.0029	1.9917	0.0698	0.0778	0.0027	1089	16	1113	24	1142	68	95
DR21-1	JN20e2	44	129	2.70	-0.19	0.1853	0.0038	2.0755	0.0915	0.0835	0.0038	1096	20	1141	31	1281	89	85
DR21-1	JN20e3	25	77	2.87	-0.53	0.1957	0.0030	2.1765	0.0676	0.0818	0.0028	1152	16	1174	22	1240	66	93
DR21-1	JN20e4	55	131	2.21	-0.08	0.1879	0.0031	2.0921	0.0571	0.0813	0.0024	1110	17	1146	19	1230	57	90
DR21-1	JN20e5	816	138	0.16	0.00	0.0825	0.0008	0.6748	0.0098	0.0591	0.0009	511	5	524	6	572	34	89
DR21-1	JN20e6	106	210	1.84	0.04	0.1793	0.0023	1.9066	0.0363	0.0769	0.0015	1063	13	1083	13	1119	38	95
DR21-1	JN20e7	78	167	1.99	-0.15	0.1779	0.0019	1.9296	0.0404	0.0789	0.0017	1055	10	1091	14	1169	43	90
DR21-1	JN20e8	58	144	2.32	0.16	0.1941	0.0021	2.0957	0.0457	0.0781	0.0017	1144	11	1147	15	1150	44	99
DR21-1	JN20e9	48	114	2.20	0.07	0.1921	0.0024	2.1592	0.0539	0.0819	0.0020	1133	13	1168	17	1242	47	91
DR21-1	JN20e10	62	138	2.08	-0.05	0.1885	0.0024	2.0482	0.0473	0.0787	0.0020	1113	13	1132	16	1166	50	95
DR21-1	JN20e11	59	154	2.42	-0.90	0.1827	0.0035	1.9264	0.0748	0.0787	0.0033	1082	19	1090	26	1164	82	93
DR21-1	JN20e12	36	102	2.68	-0.06	0.1837	0.0028	2.0343	0.0578	0.0800	0.0023	1087	15	1127	20	1196	57	91
DR21-3	jl04a1	79	188	1.70	0.10	0.1906	0.0026	2.1280	0.0601	0.0814	0.0024	1125	14	1158	20	1232	58	91
DR21-3	jl04a2	166	322	1.38	-0.24	0.1880	0.0023	2.1163	0.0481	0.0814	0.0019	1110	12	1154	16	1232	45	90
DR21-3	jl04a3	178	290	1.16	-0.22	0.1816	0.0017	1.9741	0.0353	0.0787	0.0015	1076	9	1107	12	1164	38	92
DR21-3	jl04a4	207	304	1.04	0.09	0.1821	0.0024	1.9245	0.0477	0.0770	0.0021	1078	13	1090	17	1122	53	96
DR21-3	jl04a5	184	303	1.17	-0.27	0.1855	0.0015	2.0066	0.0348	0.0784	0.0014	1097	8	1118	12	1158	35	95
DR21-3	jl04a6	200	477	1.70	0.02	0.1852	0.0017	1.9553	0.0349	0.0766	0.0015	1095	10	1100	12	1110	38	99
DR21-3	jl04a7	243	265	0.78	0.06	0.1877	0.0017	2.0496	0.0355	0.0792	0.0014	1109	9	1132	12	1177	35	94
DR21-3	jl04a8	240	292	0.87	0.05	0.1963	0.0018	2.1003	0.0368	0.0776	0.0013	1156	10	1149	12	1137	35	102
DR21-3	jl04a9	152	382	1.79	0.05	0.2027	0.0017	2.2465	0.0406	0.0806	0.0015	1190	9	1196	13	1211	36	98
DR21-3	jl04a10	183	252	0.98	-0.13	0.1865	0.0022	1.9742	0.0501	0.0770	0.0018	1103	12	1107	17	1122	46	98
DR21-3	jl04a11	137	223	1.15	-0.18	0.1579	0.0018	1.5764	0.0412	0.0738	0.0020	945	10	961	16	1035	54	91
DR21-3	jl04a12	245	540	1.57	0.05	0.1932	0.0018	2.1238	0.0353	0.0788	0.0013	1139	10	1157	12	1166	33	98
DR21-3	jl04b1	159	223	1.24	0.21	0.1926	0.0017	2.1108	0.0368	0.0796	0.0014	1136	9	1152	12	1188	34	96
DR21-3	jl04b2	101	196	1.71	0.07	0.1954	0.0020	2.1567	0.0464	0.0806	0.0018	1151	11	1167	15	1211	43	95
DR21-3	jl04b3	65	139	1.88	-0.14	0.1813	0.0021	1.9814	0.0511	0.0800	0.0021	1074	11	1109	18	1198	51	90
DR21-3	jl04b4	99	153	1.35	-0.03	0.1990	0.0020	2.1642	0.0464	0.0796	0.0018	1170	11	1170	15	1187	44	99
DR21-3	jl04b5	159	276	1.53	0.17	0.1735	0.0020	1.8415	0.0423	0.0780	0.0019	1032	11	1060	15	1147	48	90
DR21-3	jl04b6	139	185	1.17	0.01	0.1987	0.0019	2.1566	0.0400	0.0785	0.0015	1168	10	1167	13	1159	37	101
DR21-3	jl04b7	172	302	1.54	-0.06	0.1772	0.0016	1.8777	0.0361	0.0766	0.0015	1052	9	1073	13	1111	39	95
DR21-3	jl04b8	121	178	1.30	-0.13	0.1731	0.0019	1.8378	0.0409	0.0773	0.0017	1029	10	1059	15	1128	45	91

TABLE 3. *CONTINUED*

Sample	Analysis	U (ppm)	Th (ppm)	^{232}Th/^{238}U	comm. Pb^{206} (%)	Radiogenic Ratios ^{206}Pb/^{238}U	1s	^{207}Pb/^{235}U	1s	^{207}Pb/^{206}Pb	1s	Age Estimates (Ma) ^{206}Pb/^{238}U	1s	^{207}Pb/^{235}U	1s	^{207}Pb/^{206}Pb	1s	conc. (%)
DR21-3	jl04b9	224	635	2.49	0.15	0.1891	0.0016	2.0600	0.0353	0.0782	0.0013	1116	9	1136	12	1151	34	97
DR21-3	jl04b10	190	150	0.70	0.00	0.1765	0.0017	1.8696	0.0348	0.0763	0.0014	1048	9	1070	12	1103	37	95
DR21-3	jl04b11	126	202	1.41	0.26	0.1881	0.0018	2.0097	0.0426	0.0773	0.0016	1111	10	1119	14	1129	42	98
DR21-3	jl04b12	141	215	1.34	0.06	0.1869	0.0018	2.0661	0.0394	0.0796	0.0015	1105	10	1138	13	1186	38	93
DR21-8	JN20k1	240	252	1.05	-0.05	0.1842	0.0037	1.9601	0.0394	0.0778	0.0014	1090	20	1102	14	1142	36	95
DR21-8	JN20k2	172	292	1.70	-0.01	0.2022	0.0037	2.2134	0.0418	0.0799	0.0014	1187	20	1185	13	1194	35	99
DR21-8	JN20k3	202	215	1.07	-0.02	0.1896	0.0035	2.0309	0.0408	0.0783	0.0013	1119	19	1126	14	1155	34	97
DR21-8	JN20k4	182	287	1.58	-0.01	0.1935	0.0030	2.1145	0.0364	0.0809	0.0014	1140	16	1154	12	1219	35	94
DR21-8	JN20k5	107	178	1.67	-0.27	0.1927	0.0031	2.1151	0.0476	0.0807	0.0018	1136	17	1154	16	1214	44	94
DR21-8	JN20k6	214	169	0.79	0.00	0.1982	0.0031	2.1313	0.0386	0.0784	0.0014	1166	16	1159	13	1157	35	101
DR21-8	JN20k7	157	306	1.96	0.04	0.1902	0.0031	2.0319	0.0402	0.0790	0.0016	1122	17	1126	14	1172	40	96
DR21-8	JN20k8	233	297	1.28	-0.03	0.1848	0.0020	1.9512	0.0305	0.0771	0.0012	1093	11	1099	11	1123	32	97
DR21-8	JN20k9	205	230	1.12	0.01	0.1920	0.0023	2.0942	0.0360	0.0797	0.0012	1132	13	1147	12	1189	31	95
DR21-8	JN20k10	132	212	1.61	-0.01	0.1954	0.0025	2.1031	0.0415	0.0794	0.0014	1150	14	1150	14	1181	36	97
DR21-8	JN20k11	133	249	1.88	0.16	0.1992	0.0028	2.2052	0.0422	0.0811	0.0015	1171	15	1183	13	1224	37	96
DR21-8	JN20k12	331	166	0.50	-0.04	0.1959	0.0023	2.1671	0.0314	0.0811	0.0011	1153	12	1171	10	1223	26	94
DR21-8	JN30B1	134	229	1.59	0.26	0.2026	0.0026	2.1310	0.0941	0.0878	0.0042	1189	14	1159	31	1378	92	86
DR21-8	JN30B2	126	252	1.85	0.22	0.1894	0.0026	1.8217	0.0830	0.0787	0.0035	1118	14	1053	30	1166	88	96
DR21-8	JN30B3	139	297	1.98	-0.04	0.2008	0.0026	2.0087	0.0851	0.0830	0.0035	1180	14	1118	29	1268	84	93
DR21-8	JN30B4	146	141	0.89	-0.64	0.1828	0.0035	1.7108	0.1158	0.0774	0.0049	1082	19	1013	44	1130	126	96
DR21-8	JN30B5	152	306	1.87	-0.11	0.1961	0.0025	1.8251	0.0909	0.0781	0.0039	1155	14	1055	33	1149	98	100
DR21-8	JN30B6	109	304	2.58	0.07	0.1941	0.0026	1.9388	0.1058	0.0819	0.0044	1143	14	1095	37	1242	105	92
DR21-8	JN30B7	190	162	0.79	0.41	0.1910	0.0021	1.9435	0.0821	0.0833	0.0035	1127	11	1096	29	1277	83	88
DR21-8	JN30B8	127	179	1.31	-0.66	0.1841	0.0037	1.5845	0.1054	0.0755	0.0056	1089	20	964	42	1082	148	101
DR21-8	JN30B9	157	187	1.11	0.30	0.1977	0.0023	1.8604	0.0817	0.0780	0.0034	1163	13	1067	29	1146	87	101
DR21-8	JN30B10	103	174	1.57	1.51	0.1724	0.0052	1.8009	0.1857	0.0918	0.0094	1025	29	1046	70	1463	195	70
DR21-8	JN30B11	146	263	1.68	-0.39	0.2002	0.0029	1.9627	0.0846	0.0834	0.0038	1177	16	1103	29	1278	89	92
DR21-8	JN30B12	163	304	1.74	-0.11	0.1792	0.0022	1.8136	0.0752	0.0837	0.0035	1063	12	1050	27	1285	82	83

TABLE 4. EMP ANALYSES FOR MINERALS FROM DR21-1 USED IN P-T CALCULATIONS

analysis no.	30 / 1 .	23 / 1 .	27 / 1 .	7 / 1 .	25 / 1 .	33 / 1 .
mineral	grt core	hbl core	plag core	grt mantle	hbl rim	plag rim
SiO_2	37.07	39.87	57.20	37.21	40.07	57.25
TiO_2	0.04	2.05	0.01	0.02	2.02	0.00
Al_2O_3	20.70	11.10	26.68	20.68	10.98	26.25
Cr_2O_3	0.00	0.00	0.01	0.04	0.00	0.04
FeO	30.32	25.13	0.07	30.80	25.20	0.17
MnO	4.23	0.49	0.01	4.27	0.49	0.00
MgO	1.67	4.94	0.00	1.24	5.14	0.00
CaO	7.12	10.64	8.98	7.05	10.63	9.02
Na_2O	0.00	1.41	6.28	0.00	1.67	6.60
K_2O	0.00	1.86	0.22	0.01	1.80	0.26
Total	101.15	97.49	99.45	101.32	98.00	99.60
no. ox.	12	23	8	12	23	8
Si	2.968	6.313	2.578	2.980	6.317	2.583
Ti	0.002	0.245	0.000	0.001	0.239	0.000
Al	1.954	2.073	1.418	1.953	2.041	1.396
Cr	0.000	0.000	0.000	0.003	0.000	0.001
Fe	2.030	3.328	0.003	2.063	3.322	0.007
Mn	0.287	0.065	0.000	0.290	0.065	0.000
Mg	0.200	1.165	0.000	0.148	1.208	0.000
Ca	0.611	1.806	0.434	0.605	1.796	0.436
Na	0.001	0.433	0.549	0.000	0.510	0.578
K	0.000	0.375	0.013	0.001	0.362	0.015
Total	8.051	15.804	4.994	8.042	15.859	5.015